Material Solutions to Increase the Information Density in Mold-Based Production Systems

7

Maximilian Rudack, Iris Raffeis, Frank Adjei-Kyeremeh, Sayan Chatterjee, Uwe Vroomen, Andreas Bührig-Polaczek, Marie-Noemi Bold, Johannes Henrich Schleifenbaum, Julia Janowitz, Carsten Vogels, Christian Kalscheuer, Hendrik Heinemann, Marco Carlet, Kirsten Bobzin, Sönke Vogel, Arnold Gillner, Felix Melzer, Rainer Dahlmann, and Christian Hopmann

Contents

M. Rudack (✉) · I. Raffeis (✉) · F. Adjei-Kyeremeh (✉) · S. Chatterjee (✉) · U. Vroomen
A. Bührig-Polaczek
Foundry Institute, RWTH Aachen University, Aachen, Germany
e-mail: M.Rudack@gi.rwth-aachen.de; i.raffeis@gi.rwth-aachen.de; f.kyeremeh@gi.rwth-aachen.de; s.chatterjee@gi.rwth-aachen.de; u.vroomen@gi.rwth-aachen.de; sekretariat@gi.rwth-aachen.de

M.-N. Bold (✉) · J. H. Schleifenbaum
Institute for Digital Additive Production (DAP), RWTH Aachen University, Aachen, Germany
e-mail: marie-noemi.bold@dap.rwth-aachen.de; johannes.henrich.schleifenbaum@dap.rwth-aachen.de

J. Janowitz (✉) · C. Vogels (✉) · C. Kalscheuer · H. Heinemann · M. Carlet · K. Bobzin
Surface Engineering Institute (IOT), RWTH Aachen University, Aachen, Germany
e-mail: Janowitz@iot.rwth-aachen.de; vogels@iot.rwth-aachen.de; kalscheuer@iot.rwth-aachen.de; heinemann@iot.rwth-aachen.de; carlet@iot.rwth-aachen.de; info@iot.rwth-aachen.de

S. Vogel (✉) · A. Gillner
Laser Technology (LLT), RWTH Aachen University, Aachen, Germany
e-mail: soenke.vogel@llt.rwth-aachen.de; arnold.gillner@llt.rwth-aachen.de

F. Melzer (✉) · R. Dahlmann · C. Hopmann
Institute for Plastics Processing (IKV), RWTH Aachen University, Aachen, Germany
e-mail: Felix.Melzer@ikv.rwth-aachen.de; rainer.dahlmann@ikv.rwth-aachen.de; office@ikv.rwth-aachen.de

C. Brecher et al. (eds.), *Internet of Production*, Interdisciplinary Excellence Accelerator Series, https://doi.org/10.1007/978-3-031-44497-5_21

Abstract

Production processes for the manufacturing of technical components are enabled by the availability and use of adequate engineering materials. Within the Internet of Production this work stream is dedicated to developing material and process-based solutions to increase the data availability during the manufacturing and operation of discontinuous mold-based production systems such as high-pressure die casting (HPDC) and injection molding (IM). This includes the development of data-driven alloy design strategies for additively manufactured mold components using tool steels as an initial use case as well as new surface-based smart sensor and actuator solutions. Material data and properties are tracked from the steel powder production via gas atomization until the final use in a mold to produce castings. Intermediate steps include the 3D printing of mold components via laser powder bed fusion and subsequent application of physical vapor deposition and thermal spraying-based smart multilayer coatings with sensor and actuator capabilities. The coating system is refined by selective laser patterning to facilitate the integration onto complex shape molding tool surfaces. Furthermore, molecular dynamics simulation-based methods are developed to derive material properties required for the modeling of polymer-based materials. By using this integrated methodology with the application of integrated computational materials engineering (ICME) methods from the metal powder for the mold printing up until the casting or molding process, the foundation for a holistic life cycle assessment within the integrated structural health engineering (ISHE) framework is laid for the produced tooling systems as well as the molded parts.

7.1 Introduction

Mold-based production systems are of high prevalence in the manufacturing industry due to their ability to facilitate the high-volume production of technical components from material classes such as non-ferrous alloys and polymers. High-pressure die casting as well as injection molding machines are highly automated production systems that can provide a wide range of data via their sensors and control systems, especially if the process data is available via state-of-the-art interfaces such as OPC UA. Most of the direct physical interaction however happens between the mold and the process material. Consequently, the mold and its manufacturing process must become a part of the data stream within the IoP by using adequate materials and material models during mold manufacturing and the mold usage cycle. Most hot work tool steel alloy compositions that are in use for permanent molds in these processes have been optimized for the classical production route via forging, milling, and consecutive heat treatment. With the increasing adaption of 3D metal printing and its specific thermal regime rapid

development of optimized or new alloys via ICME methodologies is required to realize cost and performance goals. By capturing and storing the process data during metal powder atomization as well as the printing process the knowledge of local microstructural defects that negatively impact the properties of the mold component can be leveraged to drive ISHE-based methods to better assess the state of the mold during the usage cycle where thermal and tribo-chemical wear can occur. A key requirement to apply ICME calculations to predict the microstructural features of a cast alloy is the availability of precise information about the conditions at the mold interface to assign adequate boundary conditions for the simulation. In order to provide the required boundary conditions thin multilayer coating-based smart sensors and actuators produced by means of physical vapor deposition and thermal spraying are under development to increase the availability of data and to control the process temperature at the interface between the melt and the mold. The multilayer sensor coating system is structured by selective localized laser ablation of specific layers to enable localized functionality on AM manufactured and conventionally manufactured molds. Process data is collected for the coating as well as the laser ablation procedure to improve the sensor manufacturing process and to provide the data basis to facilitate ISHE assessments during the usage cycle of the mold. By addressing the key challenges of new material solutions for the tooling itself as well as increasing the availability of data from the mold-melt interface two crucial steps toward enabling ISHE and ICME for the mold-based production route are taken. Consequently, the digital description of the molding material itself is the remaining challenge to be overcome to facilitate ISHE and ICME from the tool steel powder until the final product from the materials engineering perspective. Molecular dynamics simulations are integrated into the IoP framework to increase the availability of material data for improved ISHE assessments of the molded part.

7.2 Powder and Alloy Development for Additive Manufacturing

Material properties of technical components must be tailored to suit specific application requirements. In conventional processing, materials are typically made to undergo multi-stage heat treatments resulting in customized microstructures. Such processes are characterized by the presence of multi-phases and their associated formation temperatures. However, a similar approach is not easily transferable to the domain of additive manufacturing (AM) due to the manifestation of metastable conditions resulting from different temperature profiles and often leading to poor component properties through defects. Therefore, a new approach to AM process-based solutions is crucial in designing materials with tailored microstructures and predictable properties that fit specific application requirements. The approach must be data-centric, where data from both the material design process and online

sensor-based measurement systems can be effectively extracted and transformed into structured and semi-structured databases with advanced querying capabilities. Subsequently, such databases can be combined with data science and AI-based approaches to analyze and exploit the optimization potentials of AM processes. Such analyses can be used to draw process-specific correlations, track material information over time, integrate predictive capabilities into the AM process chain to draw conclusions about the material microstructure and predict failures (the ISHE concept) during the product life cycle, and the computational development of alloys (the ICME concept).

Laser powder bed fusion (LPBF) is an additive manufacturing process based on the layer-wise production in a powder bed and the selective melting of the powder by means of a laser beam. Cooling rates in LPBF typically lie between 10^6 and 10^7 K/s. Investigations of LPBF manufacturability of hot work tool steels (HWTS) are limited so far, in some cases with contradictory results in microstructure-property correlations (Casati et al. 2018; Huber et al. 2019). In this work, a holistic methodology for modifying HWTS for increased LPBF-manufacturability is demonstrated with a standard 1.2343 HWTS for a mold based high-pressure die casting (HPDC) production system. First, LPBF process parameters are developed for the standard 1.2343 alloy. In the second step, the alloy composition is adapted based on the experimental results of step one to increase manufacturability. Alloy development via research scale powder atomization and blending enables the rapid production of new alloys for AM in research quantities. Alloy development has traditionally been an iterative, time- and resource-consuming process due to the constant need for remelting, casting, and testing new alloy compositions (Koss et al. 2021). Since in most LPBF processes, pre-alloyed powders are applied, another time- and energy-consuming step of atomizing metal powders follows (Ewald et al. 2019). Our team of researchers has therefore investigated the use and proven the feasibility of powder blends (mixtures of pre-alloyed and/or elemental powders) in the context of rapid alloy development for high manganese steels (Ewald et al. 2021) and high entropy alloys (Ewald et al. 2019; Kies et al. 2020).

The amount of metal powder needed can further be reduced by switching to manufacturing processes with local powder supply: in situ mixing of powders allows rapid changes between alloy compositions and the fabrication of graded samples (Koss et al. 2021). One of these processes is extreme high-speed laser material deposition (EHLA), a technology originally developed for coating applications which has evolved to a 3D printing technology (Schaible et al. 2021). Using EHLA, more than 300 different alloy compositions can be manufactured easily within one workday. EHLA process parameters can be controlled in such a way that the dendrite arm spacing is comparable to LPBF manufactured components (Koss et al. 2021). This is an important feature in the context of alloy development for LPBF, since mechanical properties are foremost influenced by microstructure which in turn depends on the chemical composition and solidification conditions such as cooling rates (Koss et al. 2021). First unpublished investigations on 1.2343 and a modification of 1.2343 show comparable DAS values in LPBF and EHLA samples. Throughout the alloy development process (Fig. 7.1), data is collected in all steps, starting with powder atomization, including powder characterization,

Fig. 7.1 Holistic material development cycle

continuing with LPBF/EHLA manufacturing, and concluding with the investigation of microstructure and properties of the final component. The data is basis for the analysis of process-material correlations to allow process optimization and predictive microstructure and property modeling. All raw data is gathered in a data lake which acts as a central hub. The effective assimilation and restructuring of this raw data enable the development of material databases, cross-platform interfaces, and inter-workstream operability. These form the basis of ICME and ISHE (integrated structural health engineering) property prediction, the improvement of material design, and the creation of digital shadows.

Cycle 1 – Standard composition: 1–6 → 10

1–3: The HWTS 1.2343 was chosen for the application and required properties, TC phase simulation was done, the powder produced, and all data stored.

4: The atomized powder was qualified for further usage in the process chain: chemical composition, shape, and particle size distribution (PSD). The powder microstructural phases were determined and quantified: martensite, 5% retained austenite (Fig. 7.2a).

5 and 6: The alloy was LPBF-printed with different print parameters. The different microstructures and properties were investigated. For the standard steel 1.2343, a heating plate (T = 500 °C) was necessary to reduce the amount of retained austenite (RA) in the martensitic matrix from 18% to max. 1,1% (Fig. 7.2b, c).

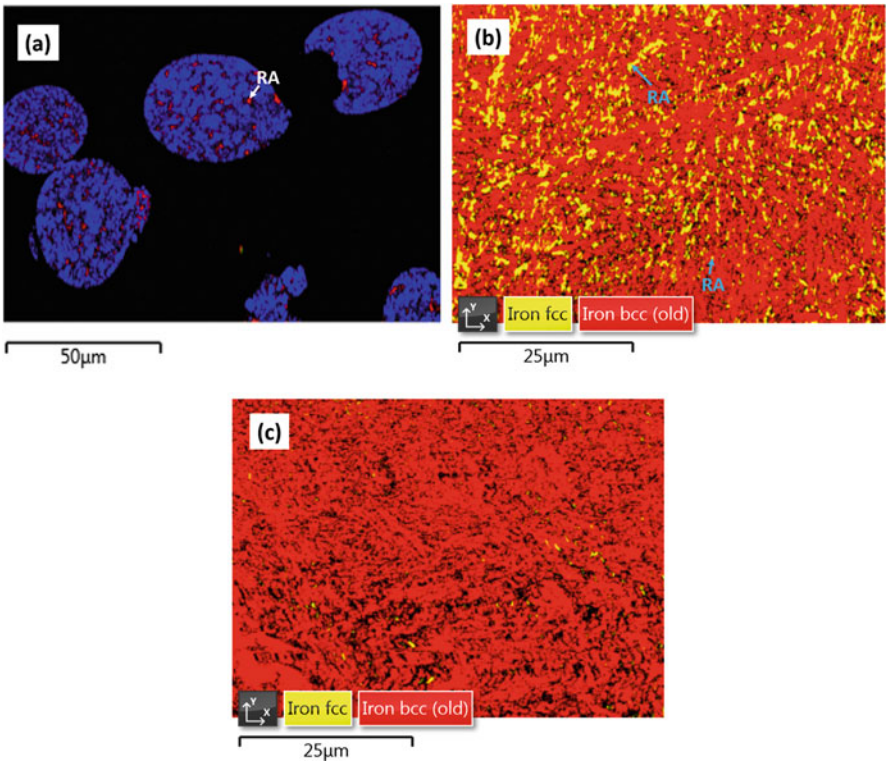

Fig. 7.2 EBSD-images of 1.2343 Standard (**a**) powder particle with ca. 5% RA (red), (**b**) as built without preheating with ca. 18% RA (yellow), (**c**) with preheating at 500 °C

Cycle 2 –Modified composition: 7, 2–6 → 10

7, 2–6: Based on findings and data gathered from 1 to 6, alloy modification was necessary with the goal to create a steel with less RA through a combination of carbon and strong carbide formers as well as solid solution strengthening alloying elements. To facilitate alloy modification and new compositional design, Calculation of phase diagrams (CALPHAD) based simulations were helpful in microstructure phases prediction (2). Based on the new modification, the alloy can either be produced via atomization or blending (3) and characterized (4). In the modification, the standard composition was adapted to the process (5). The microstructure was evaluated (grain size, cell sizes, shapes, cell boundary structures, carbides, segregations, martensitic, austenitic phases) and the mechanical properties of the printed parts with and without heat treatment were tested (6). In this modified as-built condition, no RA was found.

Correlations and property simulations: 10 → 8, 9 → 10

8: Comparison and correlations of both the steels, in terms of microstructure and mechanical properties were performed.
9: Subsequent steps would involve the simulation of material properties, the ISHE usage, and the determination of correlations among process variables.

The concept of alloy development via AM powder route supports the increased adoption of 3D printing of mold components for HPDC or IM. The main results showed that the preheated standard steel achieved the maximum strength without a second annealing treatment and that the modified steel reached its maximum strength results without a preheat treatment, both industrial benefits (Raffeis et al. 2022). Data gathered during the process chain were vital in controlling and customizing microstructures for the required property applications. The material and process data gathered along the process chain form a solid basis which shows a clear pathway for further computational alloy development leading to an alloy composition validated for manufacturing a mold for HPDC and successive smart multilayer coatings application onto the mold surface.

7.3 Smart Coatings

The temperature is an important parameter in manufacturing technology to influence tool performance and lifetime, properties of the workpiece, and energy consumption for manufacturing. For monitoring and controlling the process temperature, the data from the direct interface between mold and workpiece or mold and melt is necessary. For this purpose, a smart multilayer sensor-actor-coating-system was developed. This temperature sensor coating was deposited by means of physical vapor deposition (PVD) and combined with an actor heater coating deposited by means of thermal spraying (TS). PVD is a vacuum process. A solid target material can be transferred into gas phase by sputtering with inert gas ions, such as argon or krypton. The particles in the gas phase accelerate to the substrate, such as tools for aluminum die casting, on which the coating growth takes place. By utilization of reactive gases, such as oxygen or nitrogen, hard coatings can be deposited (Bobzin 2013). The basic principle of thermal spraying is that a feedstock material is melted with the aid of a thermal energy source (Lugscheider and Bach 2002). Subsequently, this is accelerated onto the substrate surface via an atomizing gas in the form of spray particles. On impact with the surface, which has previously been prepared and activated by blasting, the particles are flattened and solidified immediately. A coating is formed due to the overlapping of particles.

The two coating processes PVD and TS enable the deposition of coatings for the interface between mold and alumium melt. Furthermore, the deposition of the

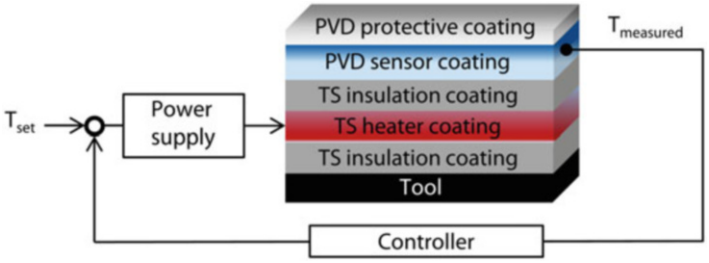

Fig. 7.3 Schematic structure of a temperature control circuit consisting of PVD temperature sensor coating and TS heater coating

required functional coatings is implemented. The schematic structure of a coating for temperature control is shown in Fig. 7.3. It composes of insulation as well as functional coatings. The electrical insulation coatings serve an electrical shielding of the functional coatings from other metallic, electrically conductive components, such as the steel tool or the molten aluminum. A further insulation coating is applied between the functional coatings to prevent electrical interference between the different principles for the sensor and actor function. The insulation top coating is in direct contact with the environment and has a protective function against wear and other stresses. The functional coatings are divided into a measuring PVD sensor and a heating TS actor coating. The measuring function, based on the operating principle of the thermoelectric effect, requires a material combination that exhibits characteristic potential differences at different temperatures (Körtvélyessy 1998). The material combination is implemented by deposition of two coatings, overlapping at the measurement position and separated at the contact positions, for measuring the differences in potential. The actuator function is based on the generation of heat on the principle of Joule heating. The metallic TS heater coating acts as a resistance heater and converts supplied electrical energy into thermal energy due to the specific electrical resistance.

The PVD sensor coating combines the function of temperature measurement with wear resistance. Metallic and nitride sensor coating variants were developed for this purpose. The nitride (Cr,Al)N + (Ti,Al)N sensor coating integrates the temperature sensing property into this protective function (Bobzin et al. 2021a). The metallic Ni + NiCr sensor coating generates a resolved potential difference, which is also used in calibrated type K thermocouples for precise temperature measurement. In combination with an aluminum oxide top insulation coating, a suitable resistance in tribological contact was provided, protecting the underlying sensor functionality (Bobzin et al. 2021b). The combination of metallic and ceramic coatings leads to the risk of an eggshell effect. Due to the reduced mechanical resistance of the metallic coatings, cracking or delamination of the insulation coating can result and affect the function of the sensor coating. The metallic sensor coatings should be applied thin to increase the ratio of wear-resistant insulation coatings to metallic coatings and to enable temperature measurement at the direct interface. Therefore, the influence

of the coating thickness on the temperature measurement by means of the metallic PVD sensor coating was considered. The parameters for deposition of the PVD sensor coatings are shown in Bobzin et al. (2021b). The coating thickness was adjusted by varying the coating time, while the other parameters were not changed. For the Ni and NiCr coatings, the deposition times $t_A = 23.75$ min for coating A, $t_B = 47.50$ min for coating B, and $t_C = 95.00$ min for coating C were varied to consider the sensor function depending on the coating thickness. The sensor function was checked by temperature measurement during the heating process in comparison to reference measurements of a calibrated type K thermocouple. The results are shown in Fig. 7.4. The calibrated thermocouple, blue, and the PVD sensor coatings A, B, and C showed an approximately constant increase in temperature up to $t = 200$ s. At $t > 200$ s the temperature control of the heating element started. The measured temperature of the calibrated thermocouple initially decreased because of convective heat transfer and readjusts with the regulation. The measured temperatures of the PVD sensor coatings were higher than the temperatures measured with the calibrated thermocouple. The temperature measurements of the PVD sensor coatings A, B, and C showed negligible differences compared to each other. The standard deviation of the individual measurements was smaller for the PVD sensor coatings compared to the calibrated thermocouple. There was good reproducibility of the measurement results regardless of the coating thickness. Accordingly, these thin PVD sensor coatings can be used in technical processes independently of the coating thickness.

Premature solidification and cold shuts of the aluminum alloy due to long flow paths in narrow sections can be prevented by an increase in the surface temperature. The TS actor coating can be used for variothermal temperature control of the cavity in die casting. In this way, the heat exchange at the interface between mold and melt can be directly influenced. The TS actor coating developed consists of several layers. A bond coating was applied to the mold, which ensures that the subsequent

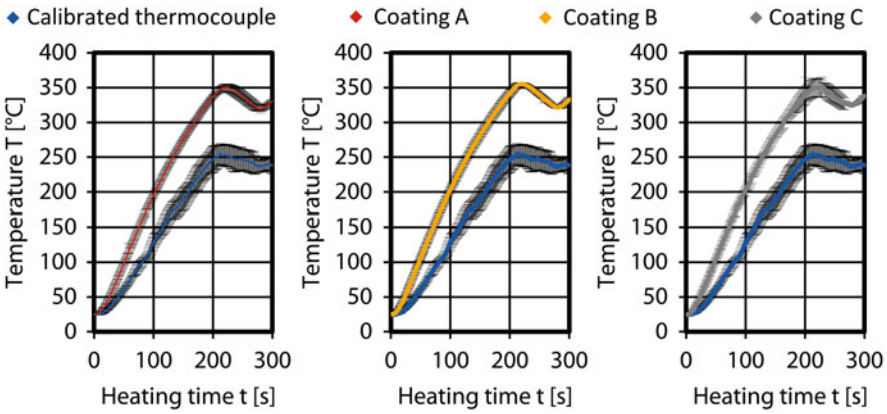

Fig. 7.4 Temperature measurement by PVD sensor coatings A, B, and C

layers adhere. For electrical insulation, the NiCr20 heater coating was surrounded by two ceramic Al_2O_3 coatings (Bobzin et al. 2021c). The applied heater coating enabled the component surface to be heated to several 100 °C. Due to the low electrical resistivity of NiCr20, the heater coating was applied in a meandering path and with a low coating thickness in order to achieve a higher electrical resistance and thus a sufficient heating power. Figure 7.5 shows a thermographic image of the heated actor coating. Up to now, heating rates of up to 10 K/s were achieved and temperatures of T = 350 °C were reached.

Both, the PVD temperature sensor coating and the TS actor coating, are functional and suitable for use in technical applications. The combination of the two coatings is the next step. Figure 7.6 shows a cross-fracture image of the combination of the metallic Ni + NiCr coatings on a TS insulation coating by scanning electron microscopy (SEM). The metallic coatings showed a columnar structure. The transition between the measuring metallic coatings was hardly visible and a suitable electrical contact for the formation of the thermoelectric effect

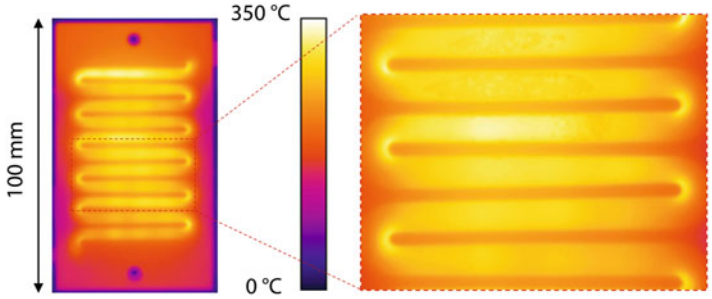

Fig. 7.5 Thermographic image of active TS actor coating

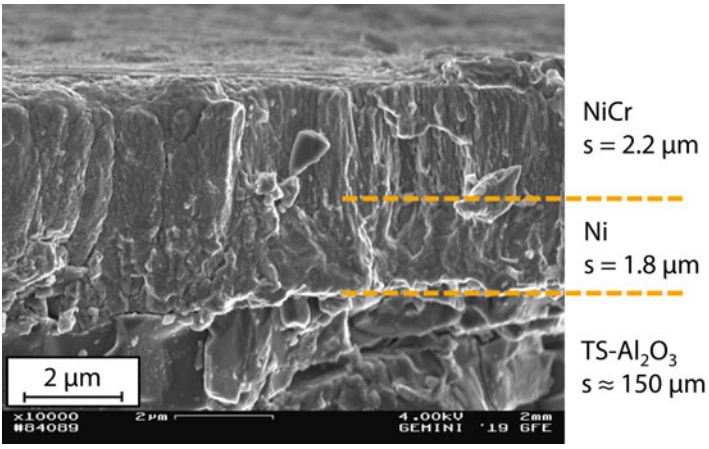

Fig. 7.6 PVD Ni + NiCr sensor on TS insulation coating in SEM cross-fraction

was assumed. No discernible gap formation between the metallic coatings and the TS insulating coating was visible. This suggests a suitable adhesion within the temperature control system. By means of the two surface technology processes, temperature monitoring and control can be implemented directly at the interface between mold and melt or between mold and workpiece. This allows an increased reliability of the mold as well as an increased component quality to be achieved.

The existing PVD sensor coating should be extended for spatially resolved measurements and the application on complex geometries. On complex geometries, masking is challenging for shaping of the contacting and measuring points. The structuring of the multilayer coating system requires a selective ablation of individual coatings without affecting the coatings underneath. In particular, the ablation of similar coatings such as the measuring sensor coatings Ni and NiCr has to be controlled and monitored precisely in the nanometer range. In this context, the extension of laser ablation offers a promising possibility, which needs to be further researched. The TS heater coating should be further improved and the heating rate increased. This can be accomplished by using a stronger power supply or increasing the electrical resistance of the heater coating through a finer meander structure. For this purpose, laser structuring can be a possibility to enable precise structuring of the heater coating.

7.4 Laser Ablation

Laser ablation is a versatile tool for thin film patterning, especially on freeform surfaces as in the present case for smart heater and sensor coatings (Fig. 7.7). Laser thin film patterning is used for different materials: transparent or opaque – dielectrics, polymers, or metals; a vast range of film and substrate material combinations is possible. The selective ablation is achieved by one of these methods: Either the processed layer is more susceptible to laser irradiation than the layer or substrate below or the laser process parameters are tuned in a trial and error method with intermediate ex-situ determination of the ablation depth and atomic composition in the ablation area. In the present case, the first method is not applicable because the threshold fluences of Ni- and NiCr-layers are identical (0.11 J/cm^2). The second method is tedious and relies on the constancy of the layer thickness. However, this assumption may fail for three-dimensional surfaces where the film deposition rate depends on local geometry features (Fig. 7.7).

Thus, we aim to measure locally and in-situ the atomic composition, identifying the currently ablated layer. Areas which have not reached the target layer are further processed. Ergo, a closed-loop control system is formed. Moreover, the gained process data is further enriched with subsequent ex-situ measurements, geometry information and data from previous process steps as depicted in Fig. 7.8. The ultimate goal is the training of an artificial intelligence (AI) with the former data. The AI is trained to optimize the laser process parameters a-priori. Laser-induced breakdown spectroscopy (LIBS) is utilized for in-situ material detection. Optical breakdown (i.e., ablation) and subsequent plasma formation of the material

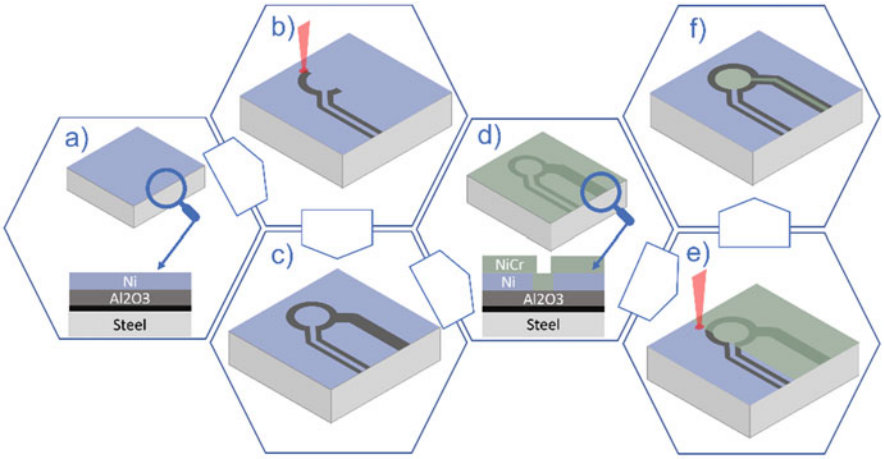

Fig. 7.7 The interplay between laser ablation and PVD coating. (**a**) The steel substrate is PVD coated with an interlay, Al_2O_3, and Ni. (**b**) Selective laser ablation of Ni to form an isolated path. (**c**) Resulting ablation pattern. (**d**) PVD coating with NiCr. (**e**) Laser ablation of NiCr. (**f**) The finished thin film sensor with a Ni and a NiCr conductor, which meet at one point to form a sensor

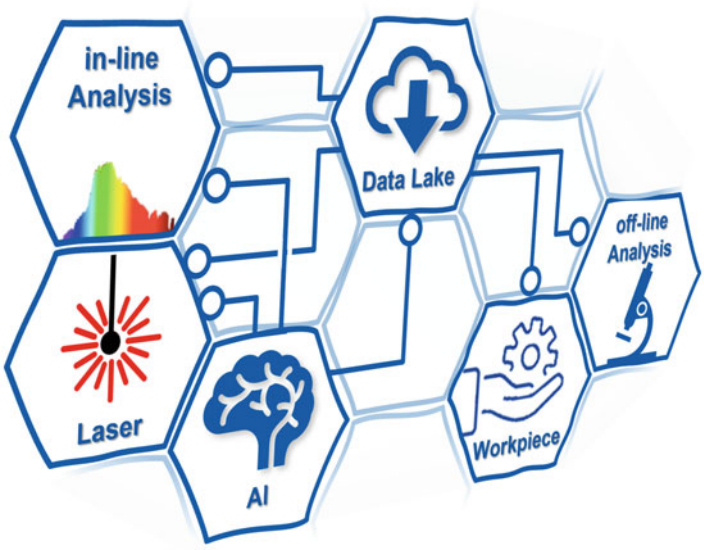

Fig. 7.8 The distributed laser process, consisting of a classical laser process, which forms a closed loop control in conjunction with an in-situ analysis. An artificial intelligence (AI), which a-priori plans the process, is constantly trained by new available data. The data is enriched by ex-situ measurements and data from the workpiece itself, such as the surface profile or the film deposition parameters. The backbone of the distributed process is a NoSQL database

are achieved by laser irradiation. The excited atoms and ions in the plasma emit characteristic line radiation (Noll 2012). LIBS has been used successfully for thin film characterization as well as depth sensing for multi-layer systems, even for sub-micrometer layer thicknesses (Nagy et al. 2017; Cabalín et al. 2011; Owens 2011).

In this work, the depth sensing capabilities of LIBS for the present film system, the two-dimensional resolution of the LIBS spectra as well as the selectivity of the ablation have been characterized. The ablation thresholds of all materials have been determined by Liu's method (1982). The film system is already described in Sect. 7.3. The depth of the ablated areas was measured with a laser scanning microscope (VK9700, Keyence) and the element ratios were determined by electron dispersive X-ray spectroscopy (EDX, Oxford Xray Detector System).

A clean ablation without damage of the isolation layer Al_2O_3 could be achieved. Even though well below the ablation threshold of Al_2O_3, the isolation layer was damaged for a fluence of 0.6 J/cm^2. The damage is attributed to spallation, induced by excessive heating of the underlying, highly absorptive TiAlN interlayer. This finding further confirms that a spatially resolved detection of the material composition is crucial for an efficient, selective process. Even a small deviation in the film thickness of Ni or NiCr could result in a damage of the isolation layer.

The depth sensing capabilities of LIBS were explored with three different methods. First, a spectrometer (HR2000+, OceanOptics) as a sensing device (He et al. 2020). The drawback of the spectrometer is its slow acquisition time of 1 ms as compared to usual laser pulse-to-pulse differences of ca. 1–10 µs. Second, a single fast photodiode was utilized. The transition from Ni to Al_2O_3 and then to steel could be determined by both methods after two and three passes. EDX was used to determine if the respective layer was completely removed. Both previous methods lack the ability to assign a signal to its spatial origin. The third method aims to overcome these drawbacks. The photodiode signal and the laser scanner (intelliScan 14 de, ScanLab) were acquired simultaneously by a custom field programmable gate array. The layer transition could be determined by all methods. However, the element composition could not be spatially resolved for the third method. Only an average difference was detected.

In conclusion, the possibility of an in-situ layer detection was shown. However, the signal needs to be spatially resolved. For that purpose, two more photodiodes will be implemented. All photodiodes will be equipped with different gauss filters, detecting single, strong emission lines of Ni, Al, and Cr. Moreover, a NoSQL database was set up and all laser parameters, ex-situ measurements, such as EDX and depth analyses, as well as the in-situ results are automatically uploaded and linked to each other. In that way all data will be at the disposal for training a deep neural network AI.

7.5 Molecular Dynamics for Digital Representation of Polymers

Plastics as polymer materials have a very wide range of properties, which can vary greatly depending on the type of polymer used. This very broad spectrum of properties leads to a high degree of complexity regarding processing and usage (Dahlmann et al. 2022). To counteract this complexity and to represent the plastic in the sense of ICME and ISHE in the cluster of excellence, the goal is to represent the polymer as a digital material and investigate in it virtually.

As Fig. 7.9 shows, the goal is to represent the plastic as a digital material, starting from its synthesis, through processing, its use in the life cycle, and the end of its lifetime by means of simulations on various scales.

In all the above stages, the complex properties of the plastic are partly or entirely determined by its molecular structure (Dahlmann et al. 2022). A simulative description of the material at the atomic level helps to represent the polymer's respectively the plastic's properties as a digital material. One important method for atomistic simulation is molecular dynamics (MD) simulation. This method relies on distributing a certain number of particles in a usually cube-shaped box. The interactions between the particles are usually described by pair potentials and their summation (Haberlandt et al. 2012).

In polyamides, the thermal properties are influenced by the corresponding water content (Batzer and Kreibich 1981). These influences can be described by MD

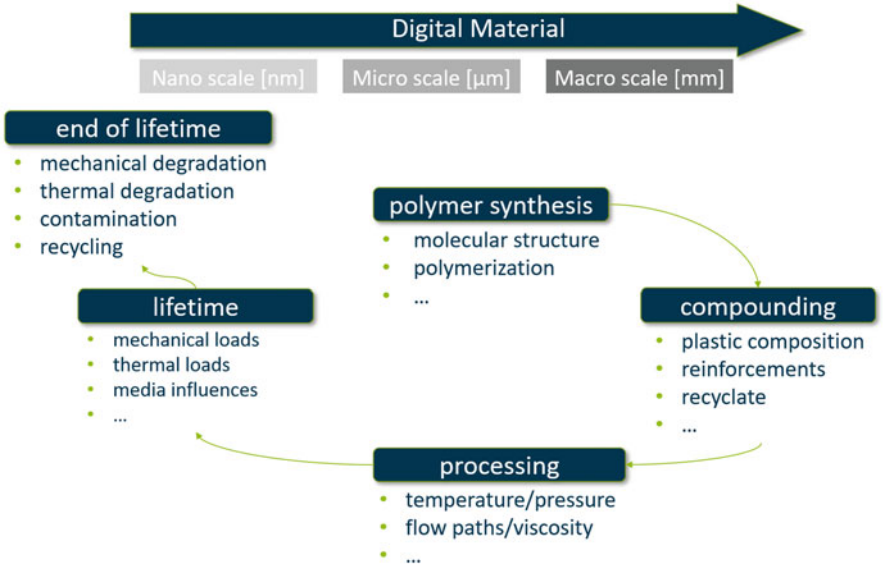

Fig. 7.9 Illustration of the plastic material throughout its complete lifecycle

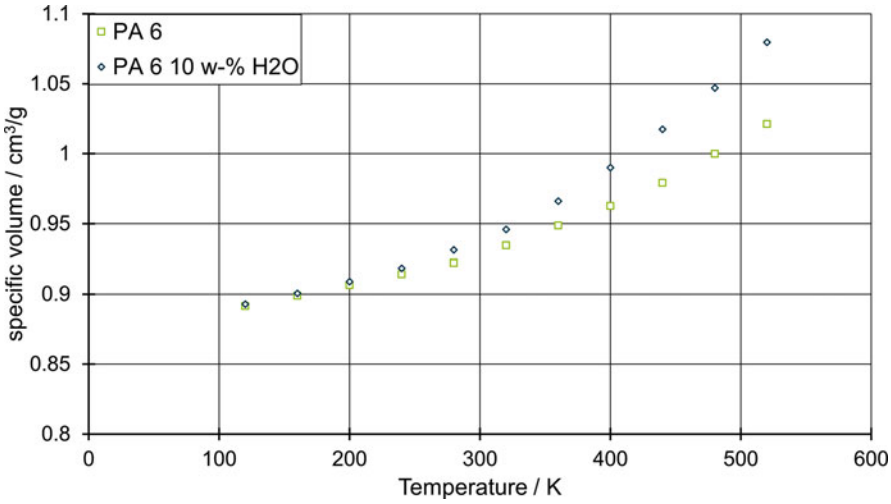

Fig. 7.10 Plotting the specific volume against temperature to investigate thermal properties of PA6 with different amounts of water uptake

simulations and thus allow their prediction. For this purpose, calculations were carried out on a dry PA6 and a PA6 saturated with 10% by weight.

As Fig. 7.10 shows, the changes in thermal behavior due to water uptake can be described, at least qualitatively, by the MD simulations. Further MD simulations were used to investigate the plastic processing, especially the process of foaming. For the modeling of the foaming process diffusion coefficients are needed which were determined by MD simulations (Melzer et al. 2022). Thus, the digital representation of the plastic material helps reduce experimental effort and reduces the needed resources. On this way plastic processing can be optimized, and sustainability is increased.

Acknowledgments Funded by the Deutsche Forschungsgemeinschaft (DFG, German Research Foundation) under Germany's Excellence Strategy – EXC-2023 Internet of Production – 390621612.

References

Batzer H, Kreibich T (1981) Influence of water on thermal transitions in natural polymers and synthetic polyamids. Polym Bull 5:585–590

Bobzin K (2013) Oberflächentechnik für den Maschinenbau. Wiley, Weinheim

Bobzin K, Brögelmann T, Kruppe NC, Janowitz J (2021a) Smart PVD hard coatings with temperature sensor function. Surf Coat Technol 423. https://doi.org/10.1016/j.surfcoat.2021.127631

Bobzin K, Kalscheuer C, Carlet M, Janowitz J (2021b) Untersuchung mehrlagiger PVD-Temperatursensorschichten unter tribologischer Beanspruchung. Paper presented at the 61st Tribologie Fachtagung

Bobzin K, Wietheger W, Heinemann H, Liao X, Vogels C (2021c) Electrical contacting of high-velocity-air-fuel sprayed NiCr20 coatings by brazing. IOP Conf Ser Mater Sci Eng 1147(1):012010

Cabalín LM, González A, Lazic V et al (2011) Deep ablation and depth profiling by laser-induced breakdown spectroscopy (LIBS) employing multi-pulse laser excitation: application to galvanized steel. Appl Spectrosc 65:797–805. https://doi.org/10.1366/11-06242

Casati R, Coduri M, Lecis N, Andrianopoli C, Vedani M (2018) Microstructure and mechanical behavior of hot-work tool steels processed by Selective Laser Melting. Mater Charact 137:50–57. https://doi.org/10.1016/j.matchar.2018.01.015

Dahlmann R, Haberstroh E, Menges G (2022) Menges Werkstoffkunde Kunststoffe. Carl Hanser, München

Ewald S, Kies F, Hermsen S, Voshage M, Haase C, Schleifenbaum JH (2019) Rapid alloy development of extremely high-alloyed metals using powder blends in laser powder bed fusion. Materials 12(10):1706

Ewald S, Köhnen P, Ziegler S, Haase C, Schleifenbaum JH (2021) Precise control of microstructure and mechanical properties of additively manufactured steels using elemental carbon powder. Mater Lett 295:129788

Haberlandt R, Fritzsche S, Peinel G, Heinzinger K (2012) Molekulardynamik – Grundlagen und Anwendungen. Braunschweig Vieweg/Teubner Verlag, Wiesbaden

He C, Gretzki P, Müller J, Gillner A, Japan Laser Processing Society (JLPS) (2020) Contribution to a conference proceedings In: Proceedings of LPM2020: 21st International Symposium on Laser Precision Microfabrication, 23–26, Dresden, Germany (Web Conference)

Huber F, Bischof C, Hentschel O, Heberle J, Zettl J, Nagulin KY, Schmidt M (2019) Laser beam melting and heat-treatment of 1.2343 (AISI H11) tool steel – microstructure and mechanical properties. Mater Sci Eng A 742:109–115. https://doi.org/10.1016/j.msea.2018.11.001

Kies F, Ikeda Y, Ewald S, Schleifenbaum JH, Hallstedt B, Körmann F, Haase C (2020) Combined Al and C alloying enables mechanism-oriented design of multi-principal element alloys: ab initio calculations and experiments. Scr Mater 178:366–371

Körtvélyessy L (1998) Thermoelement Praxis – Neue theoretische Grundlagen und deren Umsetzung. Vulkan-Verlag, Essen

Koss S, Ewald S, Bold MN, Koch JH, Voshage M, Ziegler S, Schleifenbaum JH (2021) Comparison of the EHLA and LPBF process in context of new alloy design methods for LPBF. Adv Mat Res 1161:13–25. https://doi.org/10.4028/www.scientific.net/AMR.1161.13

Liu JM (1982) Simple technique for measurements of pulsed Gaussian-beam spot sizes. Opt Lett 7:196–198. https://doi.org/10.1364/ol.7.000196

Lugscheider E, Bach FW (2002) Handbuch der thermischen Spritztechnik, Technologien – Werkstoffe – Fertigung. Verl. für Schweißen und Verwandte Verfahren DVS-Verlag, Düsseldorf

Melzer F, Breuer B, Dahlmann R, Hopmann C (2022) Calculating diffusion coefficients from molecular dynamics simulations for foam extrusion modelling of polypropylene with CO_2, N_2 and ethanol. J Cell Plast 0:1–20

Nagy TO, Pacher U, Giesriegl A et al (2017) Depth profiling of galvanoaluminium–nickel coatings on steel by UV- and VIS-LIBS. Appl Surf Sci 418:508–516. https://doi.org/10.1016/j.apsusc.2016.12.059

Noll R (2012) Laser-induced breakdown spectroscopy. Springer, Berlin/Heidelberg

Owens TN (2011) Laser induced breakdown spectroscopy and applications toward thin film analysis. Dissertation, University of California

Raffeis I, Adjei-Kyeremeh F, Ewald S, Schleifenbaum JH, Bührig-Polaczek A (2022) A combination of alloy modification and heat treatment strategies toward enhancing the properties of

LPBF processed hot working tool steels (HWTS). J Manuf Mater Process 6:63. https://doi.org/10.3390/jmmp6030063

Schaible J, Sayk L, Schopphoven T, Schleifenbaum JH, Häfner C (2021) Development of a high-speed laser material deposition process for additive manufacturing. J Laser Appl 33:012021. https://doi.org/10.2351/7.0000320